

# Nonlinear propagation equations in fibers with multiple modes—Transitions between representation bases <sup>EP</sup>

Cite as: APL Photonics 4, 022806 (2019); <https://doi.org/10.1063/1.5084118>

Submitted: 04 December 2018 . Accepted: 04 January 2019 . Published Online: 28 January 2019

C. Antonelli , A. Mecozzi , M. Shtaif , and P. J. Winzer 

## COLLECTIONS

 This paper was selected as an Editor's Pick



View Online



Export Citation



CrossMark

## ARTICLES YOU MAY BE INTERESTED IN

[Why I am optimistic about the silicon-photonic route to quantum computing](#)

APL Photonics 2, 030901 (2017); <https://doi.org/10.1063/1.4976737>

[Second harmonic generation in strained transition metal dichalcogenide monolayers: MoS<sub>2</sub>, MoSe<sub>2</sub>, WS<sub>2</sub>, and WSe<sub>2</sub>](#)

APL Photonics 4, 034404 (2019); <https://doi.org/10.1063/1.5051965>

[Entanglement distillation by Hong-Ou-Mandel interference with orbital angular momentum states](#)

APL Photonics 4, 016103 (2019); <https://doi.org/10.1063/1.5079970>

**AIP** | Conference Proceedings

Get **30% off** all  
print proceedings!

Enter Promotion Code **PDF30** at checkout



# Nonlinear propagation equations in fibers with multiple modes—Transitions between representation bases

Cite as: APL Photon. 4, 022806 (2019); doi: 10.1063/1.5084118  
Submitted: 4 December 2018 • Accepted: 4 January 2019 •  
Published Online: 28 January 2019



C. Antonelli,<sup>1</sup>  A. Mecozzi,<sup>1</sup>  M. Shtaiif,<sup>2</sup>  and P. J. Winzer<sup>3</sup> 

## AFFILIATIONS

<sup>1</sup>Department of Physical and Chemical Sciences, University of L'Aquila, L'Aquila 67100, Italy

<sup>2</sup>School of Electrical Engineering, Tel Aviv University, Tel Aviv 69978, Israel

<sup>3</sup>Nokia Bell Labs, Crawford Hill Laboratory, Holmdel, New Jersey 07733, USA

## ABSTRACT

The transverse pattern of the field that propagates in a fiber supporting multiple modes can always be described as a superposition of the patterns of the individual fiber modes. Yet, the use of other bases is often found to be more convenient, with the most famous example being that of linearly polarized modes in weakly guiding fibers. The nonlinear propagation equations contain coefficients that involve overlap integrals between the lateral profiles of multiple propagation modes. A fundamental question that has been raised in this context is whether it is legitimate to compute these coefficients from the overlap integrals between elements of alternative bases for the field representation. In this paper, we show that the answer to this question is positive in the most general sense. This result is significant in the context of space-division multiplexed transmission in multi-mode and multi-core fibers.

© 2019 Author(s). All article content, except where otherwise noted, is licensed under a Creative Commons Attribution (CC BY) license (<http://creativecommons.org/licenses/by/4.0/>). <https://doi.org/10.1063/1.5084118>

## I. INTRODUCTION

Nonlinear propagation in multi-mode optical fibers has become a subject of utmost importance in the context of space-division multiplexing (SDM) in fiber-optic communications systems. A comprehensive review and the derivation of the underlying coupled nonlinear Schrödinger equations (NLSEs) that govern propagation in ideal multi-mode fibers has been published in Refs. 1–3, whereas the more realistic case of long fibers in which significant random mode coupling occurs was treated in Refs. 4–7, where the coupled nonlinear Schrödinger equations are shown to reduce to the simpler form of coupled multi-component Manakov equations. In both cases, the parameters appearing in the equations that govern the nonlinear propagation properties involve the computation of overlap integrals between the various modes. Yet, while the fiber modes rigorously form a basis for all the spatial patterns that can be transmitted in the fiber channel, it is often convenient to consider alternative bases for describing the field evolution. A famous example is the concept of linearly polarized (LP) modes, which are used almost exclusively

when considering propagation in realistic—weakly guiding—communications fibers.<sup>8</sup> The LP modes are not true modes of the fiber in the sense that, even in the case of ideal fibers, these modes couple into each other during propagation. Another relevant example is the one of multi-core fibers with weakly coupled cores,<sup>9</sup> where the use of the modes of the individual cores—the local modes—is often preferred over the use of the true modes of the fiber structure.<sup>10</sup> Here too, the local modes are not true modes and they couple into each other during propagation.<sup>11</sup> The question that presents itself is whether it is acceptable to use the coupled multimode nonlinear Schrödinger equations<sup>1–3</sup> or the multi-component Manakov equations,<sup>4–7</sup> with nonlinearity coefficients that are computed from the overlap integrals of lateral profile functions that do not correspond to true fiber modes. This question has been addressed recently in Ref. 12 specifically in the context of the LP description of SDM fibers, and it was shown that using the expressions for the LP<sub>11</sub> lateral profile functions derived within the weakly guiding approximation<sup>8</sup> produces, in the strong coupling regime, where propagation is described

by the multi-component Manakov equation,<sup>4</sup> the same results as those obtained with the true fiber modes (TE, TM, and HE<sub>21</sub>). In this paper, we rigorously show that this is a general property, which is not restricted to the strong coupling regime, and does not need to be tested for each alternative basis separately. We prove that any set of lateral functions that is obtained from a unitary superposition of the true fiber modes is a legitimate basis for extracting the coefficients of nonlinear propagation. This statement is correct regardless of the weakly guiding approximation, and it is certainly true for the LP representation of an arbitrary number of modes. It is worth pointing out that this property has been used in Ref. 6 to predict that coupled-core multi-core fibers are characterized by a reduced nonlinear distortion as compared to parallel single-mode fibers, a result of utmost importance confirmed only recently in here SDM experiments.<sup>13,14</sup>

## II. NOTATION AND MODE BASES FOR THE ELECTRIC FIELD REPRESENTATION

We express the electric field propagating in the optical fiber as

$$\vec{E}(\vec{r}, t) = \text{Re} \left[ \sum_n \frac{\vec{F}_n(x, y, \omega_0)}{\mathcal{N}_n(\omega_0)} E_n(z, t) e^{-i\omega_0 t} \right], \quad (1)$$

where  $z$  is the propagation coordinate,  $\omega_0$  is the central optical frequency,  $n$  is the mode index, and  $E_n(z, t)$  is the corresponding complex field envelope. By  $\vec{F}_n(x, y, \omega_0)$ , we denote the lateral profile of the  $n$ th mode, i.e., the dependence of the generally three-component electric field vector on the transverse fiber coordinates, and  $\mathcal{N}_n(\omega_0)$  is a normalization coefficient that is used to ensure that  $|E_n(z, t)|^2$  is the power (in watts) carried by the  $n$ th mode. In Eq. (1), we use the fact that the signal bandwidth is much narrower than the central frequency  $\omega_0$  and that the frequency dependence of the mode lateral profiles (and consequently of the normalization constants—see below) is negligible within the signal bandwidth. The lateral profiles of the modes are mutually orthogonal according to the following definition of orthogonality:<sup>15</sup>

$$\int dx dy (\vec{F}_n \times \vec{G}_m^*) \cdot \hat{z} = 2\mathcal{N}_n^2 \delta_{n,m}, \quad (2)$$

where  $\vec{G}_n$  is the lateral profile function of the magnetic field in the  $n$ th fiber mode,  $\delta_{n,m}$  is the Kronecker delta, and  $\hat{z}$  denotes a unit-length vector pointing in the field propagation direction. This relation implies that the following weaker relation which is used for the extraction of the nonlinear propagation equations<sup>2,3,6</sup> is also satisfied:

$$\int dx dy (\vec{F}_n \times \vec{G}_m^* + \vec{F}_m^* \times \vec{G}_n) \cdot \hat{z} = 4\mathcal{N}_n^2 \delta_{n,m}. \quad (3)$$

The derivation of Eq. (2) in the absence of mode degeneracy can be found in Ref. 15, and its extension to the case of degenerate modes is presented in the Appendix of this work.

By defining normalized lateral profiles as

$$\vec{f}_n(x, y, \omega_0) = \frac{\vec{F}_n(x, y, \omega_0)}{\sqrt{2}\mathcal{N}_n}, \quad (4)$$

$$\vec{g}_n(x, y, \omega_0) = \frac{\vec{G}_n(x, y, \omega_0)}{\sqrt{2}\mathcal{N}_n}, \quad (5)$$

Eqs. (1) and (2) simplify to

$$\vec{E}(\vec{r}, t) = \sqrt{2} \text{Re} \left[ \sum_n \vec{f}_n(x, y, \omega_0) E_n(z, t) e^{-i\omega_0 t} \right], \quad (6)$$

$$\int dx dy (\vec{f}_n \times \vec{g}_m^*) \cdot \hat{z} = \delta_{n,m}. \quad (7)$$

The electric field in Eq. (6) is expressed in terms of the true fiber modes, which implies that in the absence of propagation effects, the complex envelopes evolve according to the following simple equation:

$$\frac{\partial \tilde{E}_n}{\partial z} = i\beta_n \tilde{E}_n, \quad (8)$$

where by the tilde we denote a Fourier transform,  $\tilde{s}(\omega) = \int_{-\infty}^{+\infty} s(t) \exp(i\omega t) dt$ . A point which is relevant to the present work is that the lateral profiles of the fiber modes form just one basis for the representation of any propagating field's cross section. In fact, any other basis whose elements are obtained as a unitary transformation of the lateral profile functions of the modes would work as well. However, in the latter case, the basis elements would not be propagation eigenstates, and they would couple even in the ideal case of an unperturbed fiber. To illustrate this situation, we consider the group of optical fiber modes HE<sub>21</sub><sup>even</sup>, HE<sub>21</sub><sup>odd</sup>, TM<sub>01</sub>, and TE<sub>01</sub>, which have very similar propagation constants and hence are usually referred to as quasi-degenerate,<sup>16</sup> and define four lateral profiles using the following unitary transformation:

$$\vec{f}_{\text{LP}_{\text{lix}}^{\text{even}}} = \frac{1}{\sqrt{2}} (\vec{f}_{\text{HE}_{21}^{\text{even}}} + \vec{f}_{\text{TM}_{01}}), \quad \vec{f}_{\text{LP}_{\text{lix}}^{\text{odd}}} = \frac{1}{\sqrt{2}} (\vec{f}_{\text{HE}_{21}^{\text{odd}}} + \vec{f}_{\text{TE}_{01}}), \quad (9)$$

$$\vec{f}_{\text{LP}_{\text{liy}}^{\text{even}}} = \frac{1}{\sqrt{2}} (\vec{f}_{\text{HE}_{21}^{\text{odd}}} - \vec{f}_{\text{TE}_{01}}), \quad \vec{f}_{\text{LP}_{\text{liy}}^{\text{odd}}} = \frac{1}{\sqrt{2}} (\vec{f}_{\text{HE}_{21}^{\text{even}}} - \vec{f}_{\text{TM}_{01}}), \quad (10)$$

which can be conveniently expressed as

$$\begin{bmatrix} \vec{f}_{\text{LP}_{\text{lix}}^{\text{even}}} \\ \vec{f}_{\text{LP}_{\text{lix}}^{\text{odd}}} \\ \vec{f}_{\text{LP}_{\text{liy}}^{\text{even}}} \\ \vec{f}_{\text{LP}_{\text{liy}}^{\text{odd}}} \end{bmatrix} = \frac{1}{\sqrt{2}} \begin{bmatrix} 1 & 0 & 1 & 0 \\ 0 & 1 & 0 & 1 \\ 0 & 1 & 0 & -1 \\ 1 & 0 & -1 & 0 \end{bmatrix} \begin{bmatrix} \vec{f}_{\text{HE}_{21}^{\text{even}}} \\ \vec{f}_{\text{HE}_{21}^{\text{odd}}} \\ \vec{f}_{\text{TM}_{01}} \\ \vec{f}_{\text{TE}_{01}} \end{bmatrix} = \mathbf{C} \begin{bmatrix} \vec{f}_{\text{HE}_{21}^{\text{even}}} \\ \vec{f}_{\text{HE}_{21}^{\text{odd}}} \\ \vec{f}_{\text{TM}_{01}} \\ \vec{f}_{\text{TE}_{01}} \end{bmatrix}, \quad (11)$$

where the unitary matrix  $\mathbf{C}$  defined through the second equality describes the change of basis, connecting the LP and true-mode representations. By using the above in Eq. (1), the corresponding complex envelopes are obtained in the following form:

$$\begin{bmatrix} \tilde{E}_{\text{LP}_{\text{lix}}^{\text{even}}} \\ \tilde{E}_{\text{LP}_{\text{lix}}^{\text{odd}}} \\ \tilde{E}_{\text{LP}_{\text{liy}}^{\text{even}}} \\ \tilde{E}_{\text{LP}_{\text{liy}}^{\text{odd}}} \end{bmatrix} = \mathbf{C} \begin{bmatrix} \tilde{E}_{\text{HE}_{21}^{\text{even}}} \\ \tilde{E}_{\text{HE}_{21}^{\text{odd}}} \\ \tilde{E}_{\text{TM}_{01}} \\ \tilde{E}_{\text{TE}_{01}} \end{bmatrix}. \quad (12)$$

The new lateral profiles are the ones defined by Gloge.<sup>8</sup> One can check that they too fulfill the orthogonality condition

(2), and they become linearly polarized in the weakly guiding limit, which justifies the choice of denoting them by the letters LP, as is schematically shown in Fig. 1. Note however that

treating the LP modes as truly degenerate is only an approximation, whereas in reality they evolve according to the following equation:

$$\frac{\partial}{\partial z} \begin{bmatrix} \tilde{E}_{LP_{11x}}^{even} \\ \tilde{E}_{LP_{11y}}^{even} \\ \tilde{E}_{LP_{11x}}^{odd} \\ \tilde{E}_{LP_{11y}}^{odd} \end{bmatrix} = i\mathbf{C} \begin{bmatrix} \beta_{HE_{21}} & 0 & 0 & 0 \\ 0 & \beta_{HE_{21}} & 0 & 0 \\ 0 & 0 & \beta_{TM_{01}} & 0 \\ 0 & 0 & 0 & \beta_{TE_{01}} \end{bmatrix} \mathbf{C}^\dagger \begin{bmatrix} \tilde{E}_{LP_{11x}}^{even} \\ \tilde{E}_{LP_{11y}}^{even} \\ \tilde{E}_{LP_{11x}}^{odd} \\ \tilde{E}_{LP_{11y}}^{odd} \end{bmatrix} = \frac{i}{2} \begin{bmatrix} \beta_{HE_{21}} + \beta_{TM_{01}} & 0 & 0 & \beta_{HE_{21}} - \beta_{TM_{01}} \\ 0 & \beta_{HE_{21}} + \beta_{TE_{01}} & \beta_{HE_{21}} - \beta_{TE_{01}} & 0 \\ 0 & \beta_{HE_{21}} - \beta_{TE_{01}} & \beta_{HE_{21}} + \beta_{TE_{01}} & 0 \\ \beta_{HE_{21}} - \beta_{TM_{01}} & 0 & 0 & \beta_{HE_{21}} + \beta_{TM_{01}} \end{bmatrix} \begin{bmatrix} \tilde{E}_{LP_{11x}}^{even} \\ \tilde{E}_{LP_{11y}}^{even} \\ \tilde{E}_{LP_{11x}}^{odd} \\ \tilde{E}_{LP_{11y}}^{odd} \end{bmatrix}, \quad (13)$$

which is obtained by combining Eqs. (8) and (12) and by using the unitarity property  $\mathbf{C}\mathbf{C}^\dagger = \mathbf{I}$ . Equation (13) shows that the four modes are coupled in pairs (specifically, coupling involves pairs that are formed by the same pair of true modes), and hence even if only one of them is excited at the fiber input, other modes are excited in the process of propagation and hence the field lateral profile changes, contrary to what happens with true modes.<sup>17</sup> As an example, if one excites  $LP_{11x}^{even}$  at the fiber input ( $z = 0$ ), then both the modes  $LP_{11x}^{even}$  and  $LP_{11y}^{odd}$  will be excited as follows:

$$\tilde{E}_{LP_{11x}}^{even} = e^{i\beta_0 z} \cos(\Delta\beta z) \tilde{E}_{in}, \quad (14)$$

$$\tilde{E}_{LP_{11y}}^{odd} = ie^{i\beta_0 z} \sin(\Delta\beta z) \tilde{E}_{in}, \quad (15)$$

where  $\tilde{E}_{in}$  is the input excitation,  $\beta_0 = (\beta_{HE_{21}} + \beta_{TM_{01}})/2$ , and  $\Delta\beta = (\beta_{HE_{21}} - \beta_{TM_{01}})/2$ . In this situation, the field propagating along the fiber is proportional to

$$\cos(\Delta\beta z) \vec{f}_{LP_{11x}}^{even}(x, y) + i \sin(\Delta\beta z) \vec{f}_{LP_{11y}}^{odd}(x, y), \quad (16)$$

which shows that the field's lateral profile evolves along the fiber from the shape of a pair of vertical kidneys ( $LP_{11x}^{even}$ ) at  $\Delta\beta z = k\pi$ , to that of a pair of horizontal kidneys at  $\Delta\beta z = (2k + 1)\pi/2$ , and to that of a doughnut at  $\Delta\beta z = (2k + 1)\pi/4$  ( $k = 0, 1, 2, 3, \dots$ ). This evolution is illustrated in Fig. 2.

Keeping the above discussion in mind, in what follows, we will distinguish between true fiber modes, to which we will simply refer as modes, and generic bases that can be used to represent locally the lateral profile of the field propagating along the fiber. In this context, the LP representation belongs to the latter category.

### III. BASIS INDEPENDENCE OF NONLINEAR PROPAGATION IN MULTI-MODE FIBERS

The electric field propagation in fibers is conveniently described by introducing a column vector  $\vec{E}(z, t)$  constructed by stacking the complex envelopes  $E_n(z, t)$  of locally orthogonal field distributions on top of each other. Consistent with our previous work,<sup>18</sup> we assume that the fiber supports

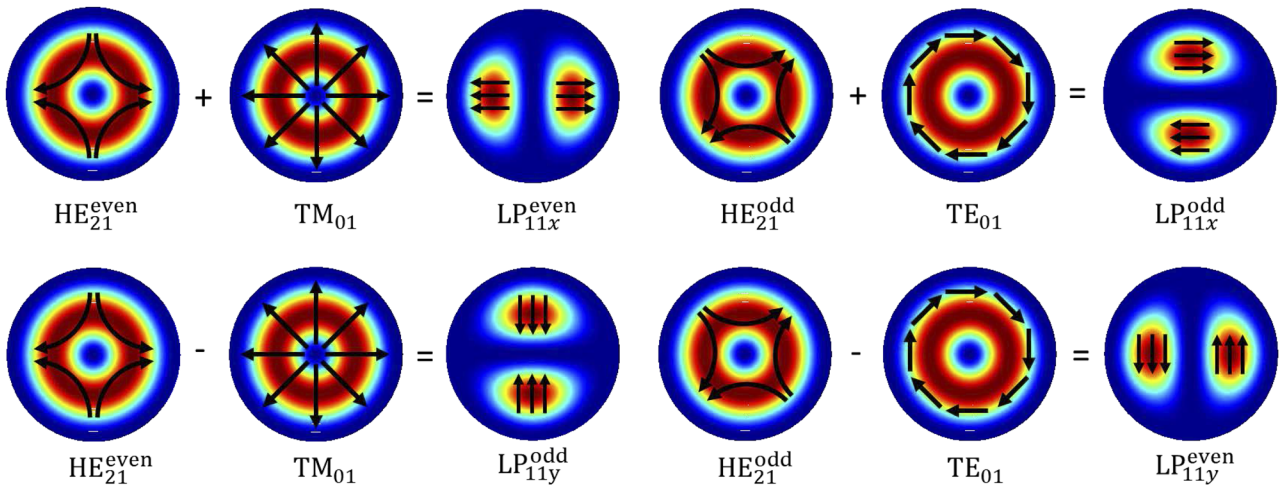


FIG. 1. The lateral profiles obtained by linearly combining those of the  $HE_{21}^{even}$ ,  $HE_{21}^{odd}$ ,  $TM_{01}$ , and  $TE_{01}$  modes of a step-index fiber are almost linearly polarized. In the regime of weak guidance, they are very close to the LP modes defined by Gloge.<sup>8,12</sup>

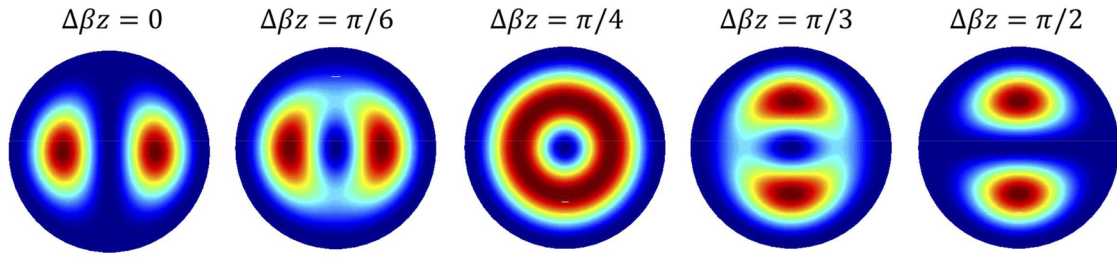


FIG. 2. Evolution of the mode lateral profile that is seen by exciting  $LP_{11x}^{\text{even}}$  only at the fiber input.

2N scalar modes. Note that while in principle the number of supported modes does not have to be even, in practice, quasi-degenerate modes, which if guided have very similar propagation constants, always come in pairs with very close cut-off frequencies (one example is the  $TM_{01}/TE_{01}$  mode pair illustrated in Sec. II), and it is practically impossible to guide only one member of that pair and suppress the other (clearly this consideration does not apply to fibers that are designed for operation in a strong guiding regime and to specialty fibers with unconventional geometry<sup>19,20</sup> and/or refractive-index profile).

We start by recalling the equation describing linear propagation in the Fourier domain, which can be expressed as

$$\frac{\partial \vec{E}}{\partial z} = -\frac{\alpha}{2} \vec{E} + i\mathbf{B}\vec{E}, \quad (17)$$

where  $\alpha$  is the fiber loss coefficient and  $\mathbf{B}(z, \omega)$  is a  $2N \times 2N$  matrix. In this work, we neglect mode-dependent loss<sup>21</sup> (MDL), in which case propagation is unitary so that  $\mathbf{B}$  is Hermitian.<sup>22-24</sup> The frequency dependence of  $\mathbf{B}$  can be adequately accounted for by a second-order Taylor expansion

$$\mathbf{B}(z, \omega) \simeq \mathbf{B}^{(0)} + \omega \mathbf{B}^{(1)} + \frac{\omega^2}{2} \mathbf{B}^{(2)}. \quad (18)$$

In ideal fibers,  $\mathbf{B}$  is diagonal in the basis of the true fiber modes, as in the example of Eq. (7), and so are its frequency derivatives. In this case, the nonzero elements of  $\mathbf{B}^{(0)}$  are the propagation constants  $\beta_n$ , those of  $\mathbf{B}^{(1)}$  are the inverse group velocities  $\beta'_n = 1/v_{g,n}$ , and those of  $\mathbf{B}^{(2)}$  are the chromatic dispersion (CD) coefficients  $\beta''_n$  of the individual modes. In real (non-ideal) fibers,  $\mathbf{B}$  typically contains non-diagonal perturbation terms that account for unavoidable manufacturing imperfections of the fiber itself as well as for mode coupling due to stress induced by cabling and deployment. Specifically,  $\mathbf{B}^{(0)}$  and  $\mathbf{B}^{(1)}$  describe position-dependent random-mode coupling and modal dispersion, respectively, whereas  $\mathbf{B}^{(2)}$  accounts for the modal dependence of the fiber chromatic dispersion. The perturbations of  $\mathbf{B}^{(2)}$  have a negligible effect relative to the effect of the perturbations in  $\mathbf{B}^{(0)}$  and  $\mathbf{B}^{(1)}$ , and hence it is legitimate to ignore the off-diagonal terms of  $\mathbf{B}^{(2)}$  in the true-mode representation.

We are now ready to introduce the coupled nonlinear Schrödinger equations, which account for linear and nonlinear

propagation phenomena

$$\begin{aligned} \frac{\partial \vec{E}}{\partial z} = & -\frac{\alpha}{2} \vec{E} + i\mathbf{B}^{(0)} \vec{E} - \mathbf{B}^{(1)} \frac{\partial \vec{E}}{\partial t} + \frac{i\mathbf{B}^{(2)}}{2} \frac{\partial^2 \vec{E}}{\partial t^2} \\ & + i\gamma \sum_n \sum_{h,k,m} C_{nhkm} E_h^* E_k E_m \hat{e}_n. \end{aligned} \quad (19)$$

The 2nd–4th terms on the right-hand side of Eq. (19) are the time-domain counterparts of the corresponding terms in Eq. (18), and the last term accounts for nonlinear propagation. The term  $\hat{e}_n$  represents a unit vector in the  $n$ th direction of the  $2N$ -dimensional field-vector space, and  $\gamma$  is the familiar fiber nonlinearity coefficient, whose expression can be found in Ref. 6. For the sake of clarity in this work, we only consider the instantaneous Kerr nonlinearity of fibers (more general equations accounting also for the Raman effect can be found in Ref. 6). In this case, the coefficients  $C_{nhkm}$  have the form<sup>6</sup>

$$C_{nhkm} = \frac{A_{\text{eff}} n_{\text{eff}}^2}{12Z_0^2} (2\mathcal{Q}_{nhkm} + \mathcal{R}_{nhkm}), \quad (20)$$

where  $A_{\text{eff}}$  and  $n_{\text{eff}}$  are the effective area and refractive index, respectively, of the fundamental mode. The terms  $\mathcal{Q}_{nhkm}$  and  $\mathcal{R}_{nhkm}$ , whose expressions were given in Ref. 6, can be rewritten as

$$\mathcal{Q}_{nhkm} = 4 \int dx dy (\vec{f}_n^* \cdot \vec{f}_m) (\vec{f}_h^* \cdot \vec{f}_k), \quad (21)$$

$$\mathcal{R}_{nhkm} = 4 \int dx dy (\vec{f}_n^* \cdot \vec{f}_h^*) (\vec{f}_m \cdot \vec{f}_k). \quad (22)$$

A subtle point that needs to be clarified relates to the fact that the coupled NLSEs are obtained by representing the field in the basis of the fiber's true modes.<sup>6</sup> In what follows, we show that the same form holds when the field is represented in a basis of lateral profile functions that are obtained from a unitary combination of the true modes, which, as discussed in the context of the LP modes example in Sec. II, are not propagation modes of the fiber (excluding cases where the true fiber modes are degenerate). In particular, we show that the expressions of the nonlinearity coefficients in Eqs. (21) and (22) do not change when transitioning from one basis to another. To this end, similarly to what we have done in Eq. (11), we introduce the  $2N \times 2N$  unitary matrix  $\mathbf{C}$  with elements  $c_{i,j}$  so that a new

set of basis functions is defined as follows

$$\vec{\varphi}_k = \sum_{l=1}^{2N} c_{k,l} \vec{f}_l, \quad \vec{\xi}_k = \sum_{l=1}^{2N} c_{k,l} \vec{g}_l. \quad (23)$$

An important property of the transformation in Eq. (23) is that the basis functions  $\vec{\varphi}_k$  and  $\vec{\xi}_k$  fulfill the orthogonality condition in Eq. (7), as can be shown by direct substitution. The corresponding inverse relations, obtained using  $\mathbf{C}\mathbf{C}^\dagger = \mathbf{I}$ , are

$$\vec{f}_k = \sum_{l=1}^{2N} c_{l,k}^* \vec{\varphi}_l, \quad \vec{g}_k = \sum_{l=1}^{2N} c_{l,k}^* \vec{\xi}_l. \quad (24)$$

We use the same matrix to define a rotated field vector  $\vec{A} = \mathbf{C}^* \vec{E}$  (note that  $\mathbf{C}^*$  is also a unitary matrix) so that

$$A_l = \sum_{k=1}^{2N} c_{l,k}^* E_k. \quad (25)$$

It can be easily checked that these definitions are consistent with the following equality between the two field expansions:

$$\sum_{n=1}^{2N} E_n \vec{f}_n = \sum_{n=1}^{2N} A_n \vec{\varphi}_n. \quad (26)$$

We now replace  $\vec{f}_k$  in Eqs. (21) and (22) with its expression in Eq. (24) and express the nonlinear term as

$$\begin{aligned} & i\gamma \frac{A_{\text{eff}} n_{\text{eff}}^2}{12Z_0^2} \sum_n \sum_{h,k,m} 4 \sum_l c_{l,k}^* \left[ 2 \int dx dy (\vec{f}_n^* \cdot \vec{f}_m) (\vec{f}_h^* \cdot \vec{\varphi}_l) \right. \\ & \quad \left. + \int dx dy (\vec{f}_n^* \cdot \vec{f}_h^*) (\vec{f}_m \cdot \vec{\varphi}_l) \right] E_h^* E_k E_m \hat{e}_n \\ & = i\gamma \frac{A_{\text{eff}} n_{\text{eff}}^2}{12Z_0^2} \sum_n \sum_{h,l,m} 4 \left[ 2 \int dx dy (\vec{f}_n^* \cdot \vec{f}_m) (\vec{f}_h^* \cdot \vec{\varphi}_l) \right. \\ & \quad \left. + \int dx dy (\vec{f}_n^* \cdot \vec{f}_h^*) (\vec{f}_m \cdot \vec{\varphi}_l) \right] E_h^* E_m \left( \sum_k c_{l,k}^* E_k \right) \hat{e}_n, \quad (27) \end{aligned}$$

and, using Eq. (25), as

$$\begin{aligned} & i\gamma \frac{A_{\text{eff}} n_{\text{eff}}^2}{12Z_0^2} \sum_n \sum_{h,l,m} 4 \left[ 2 \int dx dy (\vec{f}_n^* \cdot \vec{f}_m) (\vec{f}_h^* \cdot \vec{\varphi}_l) \right. \\ & \quad \left. + \int dx dy (\vec{f}_n^* \cdot \vec{f}_h^*) (\vec{f}_m \cdot \vec{\varphi}_l) \right] E_h^* E_m A_l \hat{e}_n. \quad (28) \end{aligned}$$

Repeating the same procedure with the expansion of  $\vec{f}_h$ ,  $\vec{f}_m$ , and  $\vec{f}_n$  yields

$$\begin{aligned} & i\gamma \frac{A_{\text{eff}} n_{\text{eff}}^2}{12Z_0^2} \sum_r \sum_{p,l,q} 4 \left[ 2 \int dx dy (\vec{\varphi}_r^* \cdot \vec{\varphi}_q) (\vec{\varphi}_p^* \cdot \vec{\varphi}_l) \right. \\ & \quad \left. + \int dx dy (\vec{\varphi}_r^* \cdot \vec{\varphi}_p^*) (\vec{\varphi}_q \cdot \vec{\varphi}_l) \right] A_p^* A_q A_l \hat{u}_r, \quad (29) \end{aligned}$$

where

$$\hat{u}_r = \left( \sum_n c_{n,r} \hat{e}_n \right). \quad (30)$$

It can be easily verified that the vectors  $\hat{u}_r$  are orthogonal unit vectors, with  $r = 1, \dots, 2N$ . More specifically, the vector  $\hat{u}_r$  describes the hyper-polarization of a field characterized by a state vector  $\vec{A}$  whose only nonzero component is  $A_r$ . As a result, the propagation equation for  $\vec{A}$  assumes the following form:

$$\begin{aligned} \frac{\partial \vec{A}}{\partial z} & = -\frac{\alpha}{2} \vec{A} + i\mathbf{C}^* \mathbf{B}^{(0)} \mathbf{C}^t \vec{A} - \mathbf{C}^* \mathbf{B}^{(1)} \mathbf{C}^t \frac{\partial \vec{A}}{\partial t} \\ & \quad + \frac{i\mathbf{C}^* \mathbf{B}^{(2)} \mathbf{C}^t}{2} \frac{\partial^2 \vec{A}}{\partial t^2} + i\gamma \sum_n \sum_{h,k,m} C_{nhkm}^{(\vec{A})} A_h^* A_k A_m \hat{u}_n, \quad (31) \end{aligned}$$

where

$$C_{nhkm}^{(\vec{A})} = \frac{A_{\text{eff}} n_{\text{eff}}^2}{12Z_0^2} \left( 2\mathcal{Q}_{nhkm}^{(\vec{A})} + \mathcal{R}_{nhkm}^{(\vec{A})} \right), \quad (32)$$

$$\mathcal{Q}_{nhkm}^{(\vec{A})} = 4 \int dx dy (\vec{\varphi}_n^* \cdot \vec{\varphi}_m) (\vec{\varphi}_h^* \cdot \vec{\varphi}_k), \quad (33)$$

$$\mathcal{R}_{nhkm}^{(\vec{A})} = 4 \int dx dy (\vec{\varphi}_n^* \cdot \vec{\varphi}_h^*) (\vec{\varphi}_m \cdot \vec{\varphi}_k) \quad (34)$$

and where we used the unitarity property  $\mathbf{C}^* \mathbf{C}^t = \mathbf{I}$ , which is obtained by taking the complex conjugate of  $\mathbf{C}\mathbf{C}^\dagger = \mathbf{I}$ . The comparison of Eqs. (32)–(34) with Eqs. (20)–(22) confirms that the nonlinearity coefficients have the same form in the two representations.

We note that the fact that the choice of representation bases has no effect on the functional form of the nonlinearity coefficients does not imply that all bases are equally convenient. In general, it is always advisable to choose a basis that best adheres to the properties of the fiber structure. This point is particularly important in the case where the fiber supports uncoupled groups of strongly coupled modes, where it would be extremely inconvenient to adopt a representation basis whose elements result from combinations of modes belonging to different groups. Even though the coupled NLSEs remain correct in this unnatural representation basis, their use would produce strong deterministic linear coupling between quasi degenerate mode groups, thereby preventing their reduction to the much simpler form of the familiar weakly coupled multi-component Manakov equations,<sup>5,6</sup> obscuring the characteristics of the propagation problem. Indeed, the coupled Manakov equations can only be obtained when each basis element in the representation can be expressed as a superposition of propagation modes belonging to a single mode-group. Moreover, the coupled Manakov equations that will be obtained with any one of such representations will have the exact same coefficients. In order to demonstrate this, we recall the expression for the averaged nonlinearity coefficients that appear in the coupled Manakov equations for two mode groups  $\mathcal{I}_j$  and  $\mathcal{I}_l$

$$\kappa_{jl} = \sum_{n \in \mathcal{I}_l} \sum_{h \in \mathcal{I}_j} \frac{C_{nhhn} + C_{nhnh}}{2N_l(2N_j + \delta_{lj})}. \quad (35)$$

The invariance of  $\kappa_{jl}$  to the choice of basis follows from the four equalities:

$$\sum_{n \in \mathcal{I}_1} \sum_{h \in \mathcal{I}_j} \mathcal{Q}_{nhhn} = \sum_{n \in \mathcal{I}_1} \sum_{h \in \mathcal{I}_j} \mathcal{Q}_{nhhn}^{(\vec{A})}, \quad \sum_{n \in \mathcal{I}_1} \sum_{h \in \mathcal{I}_j} \mathcal{R}_{nhhn} = \sum_{n \in \mathcal{I}_1} \sum_{h \in \mathcal{I}_j} \mathcal{R}_{nhhn}^{(\vec{A})}, \quad (36)$$

$$\sum_{n \in \mathcal{I}_1} \sum_{h \in \mathcal{I}_j} \mathcal{Q}_{nhnh} = \sum_{n \in \mathcal{I}_1} \sum_{h \in \mathcal{I}_j} \mathcal{Q}_{nhnh}^{(\vec{A})}, \quad \sum_{n \in \mathcal{I}_1} \sum_{h \in \mathcal{I}_j} \mathcal{R}_{nhnh} = \sum_{n \in \mathcal{I}_1} \sum_{h \in \mathcal{I}_j} \mathcal{R}_{nhnh}^{(\vec{A})}. \quad (37)$$

To prove the first, we substitute the expansion  $\vec{f}_n = \sum_{p \in \mathcal{I}_1} c_{p,n}^* \vec{\varphi}_p$  into the expression for  $\mathcal{Q}_{nhhn}$ ,

$$\begin{aligned} \mathcal{Q}_{nhhn} &= 4 \int dx dy (\vec{f}_n^* \cdot \vec{f}_n) (\vec{f}_h^* \cdot \vec{f}_h) \\ &= 4 \sum_{p,q \in \mathcal{I}_1} c_{p,n} c_{q,n}^* \int dx dy (\vec{\varphi}_p^* \cdot \vec{\varphi}_q) (\vec{f}_h^* \cdot \vec{f}_h), \end{aligned} \quad (38)$$

and using  $\sum_{n \in \mathcal{I}_1} c_{p,n} c_{q,n}^* = \delta_{pq}$ , we obtain

$$\sum_{n \in \mathcal{I}_1} \mathcal{Q}_{nhhn} = \sum_{p \in \mathcal{I}_1} \int dx dy (\vec{\varphi}_p^* \cdot \vec{\varphi}_p) (\vec{f}_h^* \cdot \vec{f}_h). \quad (39)$$

Repeating the same procedure with  $\vec{f}_h = \sum_{p \in \mathcal{I}_j} c_{p,h}^* \vec{\varphi}_p$  yields  $\sum_{n \in \mathcal{I}_1} \sum_{h \in \mathcal{I}_j} \mathcal{Q}_{nhhn} = \sum_{p \in \mathcal{I}_1} \sum_{q \in \mathcal{I}_j} \mathcal{Q}_{pqqp}^{(\vec{A})}$ . The second to fourth equalities in Eqs. (36) and (37) can be proven in a similar way, which leads to the conclusion  $\kappa_{ji} = \kappa_{ji}^{(\vec{A})}$ . This result generalizes the result obtained in Ref. 12 in the specific case of the LP<sub>11</sub> representation.

#### IV. CONCLUSIONS

The equations that govern nonlinear propagation in multi-mode fiber structures contain nonlinearity coefficients that involve overlap integrals between the lateral profile functions of the fiber modes. In this work, we have shown the legitimacy of extracting these coefficients from overlap integrals using alternative profile functions for the field representation that do not correspond to the propagation modes of the fiber, but satisfy the mode orthogonality condition. In particular, this justifies the use of the LP representation for evaluating the characteristics of nonlinear propagation in SDM systems.

#### ACKNOWLEDGMENTS

C. Antonelli and A. Mecozzi acknowledge financial support from the Italian Government under Cipe Resolution No. 135 (December 21, 2012), project INnovating City Planning through Information and Communication Technologies (INCIPICT). M. Shtaf acknowledges the support of the Israel Science Foundation Grant No. 1401/16.

#### APPENDIX: ORTHOGONALITY CONDITION FOR DEGENERATE MODES

The goal of this section is to prove the following orthogonality condition:

$$\int dx dy (\vec{F}_n \times \vec{G}_m^*) \cdot \hat{z} = 2\mathcal{N}_n^2 \delta_{n,m}, \quad (A1)$$

for two degenerate modes, namely, for two modes characterized by the same propagation constant  $\beta$ . Consistent with our previous work,<sup>6</sup> in doing so, we use the power conservation argument. This approach is more intuitive, but not less rigorous than manipulating Maxwell's equations directly.

We start by recalling that the power carried by the  $n$ th mode for an excitation characterized by the complex envelope  $E_n$  is given by

$$\begin{aligned} P_n &= \frac{1}{2} \text{Re} \left\{ \int dx dy \left( E_n \frac{\vec{F}_n}{\mathcal{N}_n} e^{i\beta z} \right) \times \left( E_n \frac{\vec{G}_n}{\mathcal{N}_n} e^{i\beta z} \right)^* \cdot \hat{z} \right\} \\ &= \frac{|E_n|^2}{4\mathcal{N}_n^2} \int dx dy (\vec{F}_{n,t} \times \vec{G}_{n,t}^* + \vec{F}_{n,t}^* \times \vec{G}_{n,t}) \cdot \hat{z}, \end{aligned} \quad (A2)$$

where in the second equality the subscript  $t$  is used to denote the transverse components of  $\vec{F}_n$  and  $\vec{G}_n$ , which are orthogonal to the propagation axis so that

$$\vec{F}_n = \vec{F}_{n,t} + F_{n,z} \hat{z}, \quad (A3)$$

$$\vec{G}_n = \vec{G}_{n,t} + G_{n,z} \hat{z}. \quad (A4)$$

If, as assumed throughout the paper, the power in watts carried by the  $n$ th mode is  $P_n = |E_n|^2$ , then the normalization constant is defined through the equality

$$\text{Re} \left\{ \int dx dy (\vec{F}_{n,t} \times \vec{G}_{n,t}^*) \cdot \hat{z} \right\} = 2\mathcal{N}_n^2. \quad (A5)$$

The  $z$ -reversal symmetry of Maxwell's equations implies that the  $z$ -reversed fields defined as

$$z\text{-reversal: } \vec{F}_n \rightarrow \vec{F}_{n,t} - F_{n,z} \hat{z}; \quad \vec{G}_n \rightarrow -\vec{G}_{n,t} + G_{n,z} \hat{z} \quad (A6)$$

also constitute a legitimate mode propagating in the backward direction. We then compute the net power flow across the fiber section when mode  $n$  and its  $z$ -reversed counterpart are both present with complex amplitudes  $E_{f,n}$  and  $E_{b,n}$ , respectively (note that  $z$ -reversal does not affect the normalization constant  $\mathcal{N}_n$ ),

$$\begin{aligned} P &= \frac{1}{2\mathcal{N}_n^2} \text{Re} \left\{ \int dx dy (E_{f,n} \vec{F}_{n,t} e^{i\beta z} + E_{b,n} \vec{F}_{n,t} e^{-i\beta z}) \right. \\ &\quad \times \left. (E_{f,n} \vec{G}_{n,t} e^{i\beta z} - E_{b,n} \vec{G}_{n,t} e^{-i\beta z})^* \cdot \hat{z} \right\} \\ &= |E_{f,n}|^2 - |E_{b,n}|^2 - \frac{1}{2\mathcal{N}_n^2} \text{Real} \left\{ e^{2i\beta z} E_{f,n} E_{b,n}^* \right. \\ &\quad \times \left. \int dx dy (\vec{F}_{n,t} \times \vec{G}_{n,t}^* - \vec{F}_{n,t}^* \times \vec{G}_{n,t}) \cdot \hat{z} \right\}. \end{aligned} \quad (A7)$$

The first and second term account for the power carried by the counter-propagating fields, whereas the third term introduces unphysical power fluctuations whose elimination yields

$$0 = \int dx dy (\vec{F}_{n,t} \times \vec{G}_{n,t}^* - \vec{F}_{n,t}^* \times \vec{G}_{n,t}) \cdot \hat{z}, \quad (A8)$$

or, equivalently,

$$\text{Im} \left\{ \int dx dy (\vec{F}_{n,t} \times \vec{G}_{n,t}^*) \cdot \hat{z} \right\} = 0. \quad (A9)$$

The above, combined with Eq. (A3), proves Eq. (A1) for  $n = m$ .

For the case  $n \neq m$ , we consider the backward propagating field constructed by applying  $z$ -reversal to the  $m$ th mode. In this case, the net power flow is given by

$$\begin{aligned} P &= \frac{1}{2} \operatorname{Re} \left\{ \int dx dy \left( E_n \frac{\vec{F}_{n,t}}{\mathcal{N}_n} e^{i\beta z} + E_m \frac{\vec{F}_{m,t}}{\mathcal{N}_m} e^{-i\beta z} \right) \right. \\ &\quad \left. \times \left( E_n \frac{\vec{G}_{n,t}}{\mathcal{N}_n} e^{i\beta z} - E_m \frac{\vec{G}_{m,t}}{\mathcal{N}_m} e^{-i\beta z} \right)^* \cdot \hat{z} \right\} \\ &= |E_n|^2 - |E_m|^2 - \frac{1}{2\mathcal{N}_n \mathcal{N}_m} \operatorname{Re} \left\{ e^{2i\beta z} E_n E_m^* \right. \\ &\quad \left. \times \int dx dy (\vec{F}_{n,t} \times \vec{G}_{m,t}^* - \vec{F}_{m,t} \times \vec{G}_{n,t}) \cdot \hat{z} \right\}, \quad (\text{A10}) \end{aligned}$$

and forcing the coefficient of  $\exp(2i\beta z)$  to zero yields

$$\int dx dy (\vec{F}_{n,t} \times \vec{G}_{m,t}^* - \vec{F}_{m,t} \times \vec{G}_{n,t}) \cdot \hat{z} = 0. \quad (\text{A11})$$

A backward propagating wave can also be constructed by using the  $t$ -reversal symmetry of Maxwell equations,

$$t\text{-reversal} : \vec{F}_n \rightarrow \vec{F}_{n,t}^* + F_{n,z} \hat{z}; \quad \vec{G}_n \rightarrow -\vec{G}_{n,t}^* - G_{n,z} \hat{z}, \quad (\text{A12})$$

which with the procedure used to obtain Eq. (A11) yields

$$\int dx dy (\vec{F}_{n,t} \times \vec{G}_{m,t} + \vec{F}_{m,t} \times \vec{G}_{n,t}) \cdot \hat{z} = 0. \quad (\text{A13})$$

Equations (A11) and (A13) do not imply Eq. (A1) yet. To make the final step, we note that application of  $z$ - and  $t$ -reversal to the  $n$ th mode yields a degenerate forward propagating mode, which we denote with  $n_c$

$$\vec{F}_{n_c} = \vec{F}_{n,t}^* - F_{n,z} \hat{z}, \quad (\text{A14})$$

$$\vec{G}_{n_c} = \vec{G}_{n,t}^* - G_{n,z} \hat{z}. \quad (\text{A15})$$

Mode  $n$  and  $n_c$  have the respective transverse components of the lateral profile functions that are the conjugate of each other, and for this reason, we refer to them as *conjugate* modes. Application of Eq. (A13) to modes  $n_c$  and  $m$  yields

$$\int dx dy (\vec{F}_{n_c,t} \times \vec{G}_{m,t} + \vec{F}_{m,t} \times \vec{G}_{n_c,t}) \cdot \hat{z} = 0, \quad (\text{A16})$$

or, equivalently,

$$\int dx dy (\vec{F}_{n,t} \times \vec{G}_{m,t}^* + \vec{F}_{m,t} \times \vec{G}_{n,t}) \cdot \hat{z} = 0. \quad (\text{A17})$$

The sum of Eqs. (A11) and (A17) gives the orthogonality condition (A1).

## REFERENCES

- <sup>1</sup>G. Agrawal, *Nonlinear Fiber Optics*, 5th ed., Optics and Photonics (Academic Press, 2013).
- <sup>2</sup>F. Poletti and P. Horak, *J. Opt. Soc. Am. B* **25**, 1645 (2008).
- <sup>3</sup>M. Kolesik and J. V. Moloney, *Phys. Rev. E* **70**, 036604 (2004).
- <sup>4</sup>A. Mecozzi, C. Antonelli, and M. Shtaif, *Opt. Express* **20**, 11673 (2012).
- <sup>5</sup>A. Mecozzi, C. Antonelli, and M. Shtaif, *Opt. Express* **20**, 23436 (2012).
- <sup>6</sup>C. Antonelli, M. Shtaif, and A. Mecozzi, *J. Lightwave Technol.* **34**, 36 (2016).
- <sup>7</sup>S. Mumtaz, R. J. Essiambre, and G. P. Agrawal, *J. Lightwave Technol.* **31**, 398 (2013).
- <sup>8</sup>D. Gloge, *Appl. Opt.* **10**, 2252 (1971).
- <sup>9</sup>R. Ryf, R. Essiambre, A. Gnauck, S. Randel, M. A. Mestre, C. Schmidt, P. Winzer, R. Delbue, P. Pupalaiakis, A. Sureka, T. Hayashi, T. Taru, and T. Sasaki, in *Optical Fiber Communication Conference* (Optical Society of America, 2012), p. PDP5C.2.
- <sup>10</sup>C. Xia, N. Bai, I. Ozdur, X. Zhou, and G. Li, *Opt. Express* **19**, 16653 (2011).
- <sup>11</sup>C. Antonelli, A. Mecozzi, and M. Shtaif, *Opt. Express* **23**, 2196 (2015).
- <sup>12</sup>F. Schmidt and K. Petermann, *J. Lightwave Technol.* **35**, 4859 (2017).
- <sup>13</sup>R. Ryf, J. C. Alvarado, B. Huang, J. Antonio-Lopez, S. H. Chang, N. K. Fontaine, H. Chen, R. J. Essiambre, E. Burrows, R. Amezcua-Correa, T. Hayashi, Y. Tamura, T. Hasegawa, and T. Taru, in *ECOC 2016-Post Deadline Paper; 42nd European Conference on Optical Communication* (IEEE, 2016), pp. 1-3.
- <sup>14</sup>R. Ryf, N. K. Fontaine, S. H. Chang, J. C. Alvarado, B. Huang, J. Antonio-Lopez, H. Chen, R. J. Essiambre, E. Burrows, R. W. Tkach, R. Amezcua-Correa, T. Hayashi, Y. Tamura, T. Hasegawa, and T. Taru, in *Proceedings of the European Conference on Optical Communication* (ECOC) (IEEE, 2017), pp. 1-3.
- <sup>15</sup>T. Tamir, E. Garmire, J. Hammer, H. Kogelnik, and F. Zernike, *Integrated Optics*, Topics in Applied Physics (Springer, Berlin, Heidelberg, 2013).
- <sup>16</sup> $HE_{21}^{\text{even}}$  and  $HE_{21}^{\text{odd}}$  mode profiles are identical and only rotated by  $45^\circ$  one with respect to the other, and hence they are rigorously degenerate. This degeneracy is caused by the cylindrical symmetry of the fiber and is absent only in modes, like  $TM_{01}$  and  $TE_{01}$ , that are rotationally invariant.
- <sup>17</sup>Note that the off-diagonal terms are propagation constant differences, and in the regime where they are negligible, the LP modes can be considered true fiber modes.
- <sup>18</sup>C. Antonelli, A. Mecozzi, M. Shtaif, and P. J. Winzer, *Opt. Express* **20**, 11718 (2012).
- <sup>19</sup>E. Ip, G. Milione, M.-J. Li, N. Cvijetic, K. Kanonakis, J. Stone, G. Peng, X. Prieto, C. Montero, V. Moreno, and J. L. nares, *Opt. Express* **23**, 17120 (2015).
- <sup>20</sup>L. Rechtman, D. M. Marom, J. S. Stone, G. Peng, and M. Li, in *2017 IEEE Photonics Conference (IPC)* (IEEE, 2017), pp. 43-44.
- <sup>21</sup>P. J. Winzer and G. J. Foschini, *Opt. Express* **19**, 16680 (2011).
- <sup>22</sup>The interplay between MDL and fiber nonlinearity is a largely unexplored subject, and its consideration goes beyond the goal of the present analysis (only isolated studies are available<sup>23,24</sup>).
- <sup>23</sup>G. Rademacher, S. Warm, and K. Petermann, *IEEE Photonics Technol. Lett.* **25**, 1203 (2013).
- <sup>24</sup>C. Xie, *Opt. Express* **19**, B915 (2011).